

CHARACTERISTICS OF LIGHT CHARGED PARTICLE EMISSION IN THE TERNARY FISSION OF ^{250}Cf AND ^{252}Cf AT DIFFERENT EXCITATION ENERGIES

S. VERMOTE[†] AND C. WAGEMANS

Department of Physics and Astronomy, University of Gent, B-9000 Gent, Belgium

O. SEROT

CEA Cadarache, DEN/DER/SPRC/LEPh, F-13108 Saint-Paul-lez-Durance, France

J. HEYSE

*SCK•CEN, Boeretang 200, B-2400 Mol, Belgium and
EC-JRC Institute for Reference Materials and Measurements, B-2440 Geel, Belgium*

T. SOLDNER* AND P. GELTENBORT

Institut Laue-Langevin, F-38042 Grenoble, France

I. ALMAHAMID

Wadsworth Center, New York State Department of Health, Albany, NY 12201, USA

G. TIAN AND L. RAO

Lawrence Berkeley National Laboratory, Berkeley, CA 94720, USA

The emission probabilities and the energy distributions of tritons, α and ^6He particles emitted in the spontaneous ternary fission (zero excitation energy) of ^{250}Cf and ^{252}Cf and in the cold neutron induced fission (excitation energy ≈ 6.5 MeV) of ^{249}Cf and ^{251}Cf are determined. The particle identification was done with suited ΔE -E telescope detectors, at the IRMM (Geel, Belgium) for the spontaneous fission and at the ILL (Grenoble, France) for the neutron induced fission measurements. Hence particle emission characteristics of the fissioning systems ^{250}Cf and ^{252}Cf are obtained at zero and at about 6.5 MeV excitation energies. While the triton emission probability is hardly influenced by the excitation energy, the ^4He and ^6He emission probability in spontaneous fission is higher than for neutron induced fission. This can be explained by the strong influence of the cluster preformation probability on the ternary particle emission probability.

[†] Corresponding author. E-mail address: sofie.vermote@ugent.be.

* Presently at Physics Department E18, TU Munich, 85748 Garching, Germany.

1. Introduction

Nuclear fission is generally a binary process. However, once every 300-400 fission events a light charged particle accompanies the two fission fragments. This process is called ternary fission.

We will focus on the characteristics of the particles with the largest emission probability, i.e. α particles (also called Long Range Alpha or LRA particles), tritons (t) and ${}^6\text{He}$ particles, for two reasons: (a) triton emission yields are needed by nuclear industry for safe manipulations of radioactive waste [1]; (b) since a different behavior of ternary α and triton emission was observed previously [2], we wanted to answer the question of how ${}^6\text{He}$ particles will behave.

Californium isotopes provide an excellent opportunity to investigate the influence of the cluster preformation probability factor, as well as the influence of the excitation energy of the compound nucleus. These effects are studied here by measuring the fissioning systems ${}^{250}\text{Cf}$ and ${}^{252}\text{Cf}$ at zero excitation energy (spontaneous fission) and at an excitation energy of about 6.5 MeV (neutron induced fission).

This paper gives an overview of the results of the study of Cf isotopes. More details can be found in [3].

2. Experimental setup

The spontaneous fission of ${}^{250,252}\text{Cf}$ has been studied at the Institute for Reference Materials and Measurements (IRMM) in Geel, Belgium. The ${}^{249,251}\text{Cf}$ neutron induced fission measurements were carried out at the PF1b cold neutron beam facility installed at the High Flux Reactor of the Institut Laue-Langevin (ILL) in Grenoble, France.

2.1. Sample characteristics

Highly enriched ${}^{249}\text{Cf}$ and ${}^{250}\text{Cf}$ samples were prepared at the Lawrence Berkeley National Laboratory in the USA. Both ${}^{251}\text{Cf}$ and ${}^{252}\text{Cf}$ samples were prepared at the Institute of Nuclear Chemistry of Mainz University in Germany. Special attention has to be given to the isotopic composition of the ${}^{251}\text{Cf}$ sample: ${}^{249}\text{Cf}$ (17.65%), ${}^{250}\text{Cf}$ (35.40%), ${}^{251}\text{Cf}$ (46.18%) and ${}^{252}\text{Cf}$ (0.77%). Due to this composition, the spontaneous fission yield and the contribution of ${}^{249}\text{Cf}(n,f)$ were not negligible.

2.2. Detection system

For the $^{249,251}\text{Cf}$ neutron induced fission measurements the sample was placed in the centre of a vacuum chamber at an angle of 45 degrees with the incoming neutron beam. For the spontaneous fission of $^{250,252}\text{Cf}$ the same setup was used, however here we measured without neutron beam, so the sample could be placed right in front of the detectors.

The measurements were performed in two separate steps. In a first step, ternary particles were detected, allowing the determination of both energy distributions and counting rates. Therefore well-calibrated silicon surface barrier detectors were used.

In addition, ΔE detectors were covered with thin aluminum foils of 25 or 30 μm to stop α decay particles and fission fragments from penetrating the detector.

For all experiments the detector characteristics were chosen in order to have the best setup for detecting α and ^6He particles (ΔE detector with a thickness between 29.8 μm and 35 μm , E detector with a thickness of 500 μm), or for detecting α particles and tritons (ΔE detector with a thickness between 41 μm and 62.9 μm , E detector with a thickness of 1500 μm).

In a second step, binary fission fragments were detected in order to determine the Binary Fission Yield (B). At this stage, the ΔE detector from the telescope suited to measure LRA/B, was removed, together with the aluminum foil, and replaced by a dummy ring with exactly the same dimensions. In this way, binary fission fragments could be measured with the E-detector (which was always thick enough) under the same detection geometry as ternary particles.

3. Measurements and results

3.1. Particle identification

The procedure used to identify various ternary particles and separate them from the background is the one proposed by Goulding et al. [4]. This method is based on the difference in energy loss of different particles in the same material using the equation: $T/a = (E + \Delta E)^{1.73} - E^{1.73}$, where T is the thickness of the ΔE detector and a is a particle and material specific constant.

The selection of ternary particles was realized by putting a window on the region of interest of the T/a spectrum. In the case of the tritons, an additional correction due to the background was needed. After the selection, ΔE and E spectra were obtained for a given ternary particle and the total energy distribution could be deduced. The thresholds in energy for each ternary particle are due to the thickness of the ΔE detector, the electronic noise and the presence

of the Al-foil. The average energy and the Full Width at Half Maximum (FWHM) of the energy distribution were obtained from a Gaussian fit performed on the experimental data.

3.2. Results

3.2.1. Binary fission

A typical binary fission spectrum is shown in Fig. 1. The alpha pile-up peak in the lowest channels due to the radioactive decay of the Cf isotope has to be removed. Then the remaining spectrum is extrapolated and the corresponding number of binary fission events can be deduced after integration of the extrapolated spectrum.

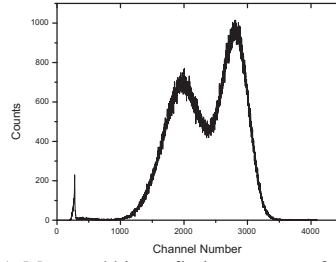


Figure 1: Measured binary fission spectrum for $^{249}\text{Cf}(n,f)$.

3.2.2. Ternary fission

Fig. 2 shows the spectra for the LRA, triton and ^6He measurements for $^{249}\text{Cf}(n,f)$. The characteristics of the energy distributions for the four Cf isotopes are given in Table 1. Emission probabilities relative to LRA particles are reported in Table 2 together with the absolute emission probabilities. All the uncertainties given correspond to the sum of statistical and systematical uncertainties.

Table 1: Values for average energy (E) and full width at half maximum (FWHM) for the various ternary particles measured.

	LRA		Tritons		^6He	
	E [MeV]	FWHM[MeV]	E [MeV]	FWHM[MeV]	E [MeV]	FWHM[MeV]
^{249}Cf	16.09 ± 0.18	10.64 ± 0.27	8.47 ± 0.19	8.52 ± 0.34	10.99 ± 0.32	10.35 ± 0.60
^{251}Cf	15.89 ± 0.12	10.60 ± 0.18	8.53 ± 0.12	8.39 ± 0.19	10.84 ± 0.36	9.98 ± 0.53
^{250}Cf	15.95 ± 0.13	10.49 ± 0.16	8.31 ± 0.30	8.58 ± 0.49	10.64 ± 0.30	10.49 ± 0.54
^{252}Cf	15.96 ± 0.09	10.22 ± 0.18	8.55 ± 0.28	8.26 ± 0.43	11.22 ± 0.52	8.95 ± 0.81

Table 2: Values for relative and absolute emission probabilities (per fission) for the various ternary particles measured.

	LRA/B [10^{-3}]	t/B [10^{-3}]	${}^6\text{He}/\text{B}$ [10^{-3}]	t/LRA [%]	${}^6\text{He}/\text{LRA}$ [%]
${}^{249}\text{Cf}$	2.77 ± 0.11	2.13 ± 0.15	6.99 ± 0.66	7.76 ± 0.50	2.54 ± 0.23
${}^{251}\text{Cf}$	2.41 ± 0.14	2.20 ± 0.14	7.58 ± 0.69	9.02 ± 0.58	3.15 ± 0.34
${}^{250}\text{Cf}$	2.93 ± 0.10	2.08 ± 0.27	8.03 ± 1.00	6.96 ± 0.89	2.74 ± 0.33
${}^{252}\text{Cf}$	2.56 ± 0.07	1.89 ± 0.19	7.68 ± 0.72	7.37 ± 0.72	3.00 ± 0.27

For LRA particles, a Gaussian fit was performed on experimental data with an energy above 12.5 MeV. In the case of tritons and ${}^6\text{He}$ particles, a Gaussian fit to all data points is performed.

Due to the isotopic composition of the ${}^{251}\text{Cf}$ sample, two measurements had to be performed in each step: one with the neutron beam open, measuring both the neutron induced fission and the spontaneous fission for all isotopes present in the sample, and one with closed neutron beam, to determine the contribution of the spontaneous fission of ${}^{250,252}\text{Cf}$. Thus, results can be derived for the neutron induced fission only. However, a correction still has to be made for the ${}^{249}\text{Cf}(\text{n},\text{f})$ contribution. This can be done easily since experimental results with the ${}^{249}\text{Cf}$ sample are available.

In addition, for ${}^{252}\text{Cf}$, a measurement without protective Al-foil before the ΔE detector was performed in order to examine the non-Gaussian tailing on the low-energy side of the energy distribution for the α particles. This measurement provided an α energy distribution with a low detection limit of 7.5 MeV (Fig. 3). Our results nicely agree with the non-Gaussian low-energy tailing observed by Tischenko et al. [5], confirmed also by Mutterer et al. [6].

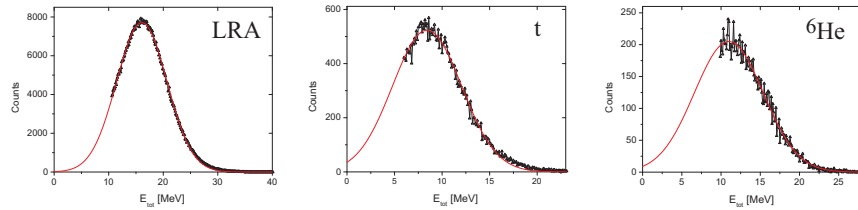


Figure 2: Energy distributions for LRA, tritons and ${}^6\text{He}$ for ${}^{249}\text{Cf}(\text{n},\text{f})$.

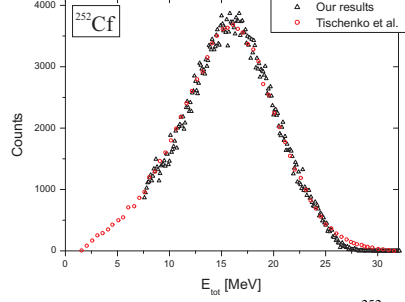


Figure 3: Energy distribution for the ternary α particles emitted in $^{252}\text{Cf}(\text{SF})$, without Al protecting foil, in comparison with the results obtained by Tischenko et al. [5].

4. Discussion

In order to search for systematic trends, we base the discussion on the californium data reported above and on similar data obtained by our research group for curium isotopes [7], for the spontaneous fission of plutonium isotopes [8] and for the thermal neutron induced fission of ^{233}U , ^{235}U , ^{239}Pu , ^{241}Pu [9], ^{237}Np [10] and ^{229}Th , ^{241}Am , ^{243}Am [11].

To examine the influence of the excitation energy on the emission probabilities, Fig. 4 is shown. In the upper left figure, the LRA emission probability is plotted as a function of the fissility parameter Z^2/A of the compound nuclei. The same is done for the tritons (Fig. 4, lower part). These figures allow several observations. First, the general trend is demonstrated that both α and triton emission probabilities increase with increasing fissility, although still strong fluctuations are seen for the α particles. Another observation is that we see a decrease of the LRA emission probability with increasing excitation energy, while the triton emission probability is hardly affected.

This difference can be explained by the strong impact of the alpha cluster preformation probability factor S_α . When the fissioning nucleus is formed after capture of a neutron, S_α is likely to decrease due to the excitation energy, in this way explaining the decrease of LRA/B. Since in the triton emission process no cluster preformation is involved, a similar effect does not occur here.

A new plot (Fig. 4, upper part, right) is made for the LRA particles, showing $(\text{LRA/B})/S_\alpha$ as a function of Z^2/A . In this figure, the strong fluctuations, shown in the left part of Fig. 4, are mostly gone, and the data vary now in a more smooth way as a function of Z^2/A as they do for tritons.

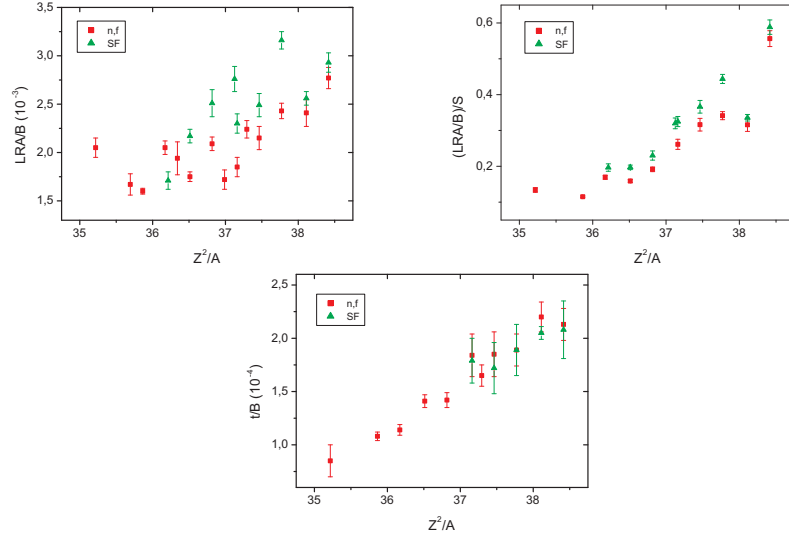


Figure 4: LRA/B (upper part, left), $(LRA/B)/S_\alpha$ (upper part, right) and t/B (lower part) as a function of Z^2/A of the compound nucleus.

Examining the behavior of ${}^6\text{He}$ particles, Fig. 5 (left) shows the absolute emission probability ${}^6\text{He}/B$ as a function of Z^2/A . Three isotope couples are plotted, namely ${}^{243}\text{Cm}(n,f) - {}^{244}\text{Cm}(\text{SF})$, ${}^{249}\text{Cf}(n,f) - {}^{250}\text{Cf}(\text{SF})$ and ${}^{251}\text{Cf}(n,f) - {}^{252}\text{Cf}(\text{SF})$. Again an indication of an increase of ${}^6\text{He}/B$ with increasing fissility is demonstrated, and in all cases a (slightly) higher value for spontaneous fission than for neutron induced fission can be observed.

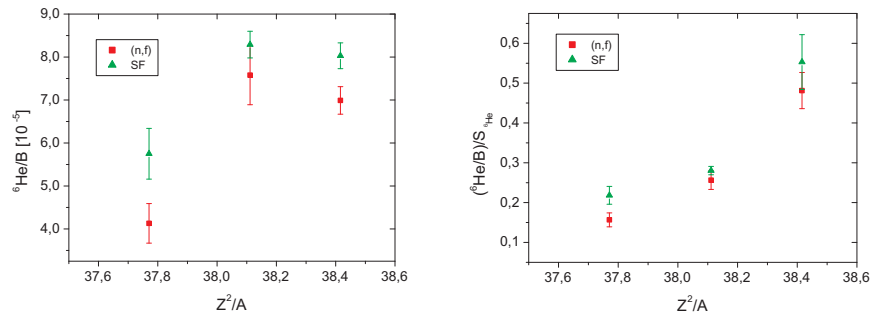


Figure 5: The absolute emission probabilities for ternary ${}^6\text{He}$ particles (left) and $({}^6\text{He}/B)/S_{{}^6\text{He}}$ (right) as a function of Z^2/A of the compound nucleus.

In analogy with the ternary α emission, a cluster preformation probability S_{He}^6 can be introduced, according to the relation proposed by Blendowske: $S_{\text{He}}^6 = S_{\alpha}^{5/3}$ [12]. The effect of S_{He}^6 is illustrated in Fig. 5 (right). It can be seen that the data suggest now to vary in a more smooth way as a function of Z^2/A , as previously observed for LRA, however further data would be helpful. The above observations permit to conclude that the ${}^6\text{He}$ particles behave more like α particles than like tritons.

In addition, the relative emission probabilities of ${}^6\text{He}$ particles provide interesting information. The absolute emission probability for α particles can be written as follows:

$$\frac{LRA}{B} = S_{\alpha} \cdot P_{LRA}$$

with P_{LRA} the probability that an α particle is emitted when it is already present in the fissioning nucleus. The same relation is valid for the ${}^6\text{He}$ particles:

$$\frac{{}^6He}{B} = S_{\text{He}}^6 \cdot P_{\text{He}}^6$$

with P_{He}^6 the probability that a ${}^6\text{He}$ particle is emitted when it is already present in the fissioning nucleus. Dividing both relations leads to:

$$\frac{{}^6He}{LRA} = \frac{S_{\text{He}}^6}{S_{\alpha}} \cdot \frac{P_{\text{He}}^6}{P_{LRA}}$$

Taking into account the above mentioned relation by Blendowske [12], we obtain:

$$\frac{{}^6He}{LRA} = S_{\alpha}^{2/3} \cdot \frac{P_{\text{He}}^6}{P_{LRA}}$$

The values of S_{α} for the different Cf isotopes vary between 10^{-2} and 10^{-3} [13], therefore the value of $S_{\alpha}^{2/3}$ is between 2.9% and 3.9%. In Table 2, it can be seen that the value of $\frac{{}^6He}{LRA}$ is between 2.54% and 3.15%. Taking into account the

uncertainties on these values, this is a clear indication that the dominating element in the determination of the relative ${}^6\text{He}$ emission probability is the

cluster preformation factor, implying that the ratio $\frac{P_{\text{He}}^6}{P_{LRA}} \cong 1$.

5. Conclusion

The present work provides experimental data on the ternary α , triton and ${}^6\text{He}$ emission for the fissioning systems ${}^{250}\text{Cf}$ and ${}^{252}\text{Cf}$ in the ground state and at an excitation energy of about 6.5 MeV. These results significantly enlarge the available ternary fission data base. Furthermore, this work puts into evidence the

strong impact of particle preformation on the ternary particle emission probability. We demonstrate first evidence that the emission probabilities for ${}^6\text{He}$ particles can be described by a preformation factor S^6_{He} . This indicates that the ${}^6\text{He}$ particles behave more like α particles than like tritons.

Acknowledgments

Part of this work was performed in the framework of the Interuniversity Attraction Poles project financed by the Belgian Science Policy Office of the Belgian State.

References

1. R. Mills, Compilation and evaluation of fission yield nuclear data, IAEA-TECDOC-1168 (2000).
2. C. Wagemans, Proc. Seminar on Fission Pont d'Oye II, Habay-la-Neuve, Belgium, 61 (1991).
3. S. Vermote et al., *Nucl. Phys.* **A837**, 176 (2010).
4. F. Goulding, D. Landis, J. Cerny and R. Pehl, *Nucl. Instr. Meth.* **31**, 1 (1964).
5. V. Tischenko, U. Jahnke, C. Herbach and D. Hilscher, Report HMI-B 588 (2002).
6. M. Mutterer et al., *Phys. Rev.* **C78**, 064616 (2008).
7. S. Vermote et al., *Nucl. Phys.* **A806**, 1 (2008).
8. O. Serot and C. Wagemans, *Nucl. Phys.* **A641**, 34 (1998).
9. C. Wagemans, P. D'hondt, P. Schillebeeckx and R. Brissot, *Phys. Rev.* **C33**, 943 (1986).
10. C. Wagemans et al., *Nucl. Phys.* **A369**, 1, 1981.
11. C. Wagemans, Proc. Int. Workshop on Dynamical Aspects of Nuclear Fission, Smolenice, Slovak Rep., E.V. Ivashkevich, 139 (1991).
12. R. Blendowske, T. Fliesbach and H. Walliser, *Z. Phys.* **A339**, 121 (1991).
13. S. Vermote, Ph.D. Thesis, University of Gent (2009).